

# Supporting Information

## Quantitative Imaging of Glutathione in Live Cells Using a Reversible Reaction-Based Ratiometric Fluorescent Probe

Xiqian Jiang,<sup>†</sup> Yong Yu,<sup>¶</sup> Jianwei Chen,<sup>†</sup> Mingkun Zhao,<sup>‡</sup> Xianzhou Song,<sup>†</sup> Alexander J. Matzuk,<sup>†</sup> Shaina L. Carroll,<sup>†</sup> Xiao Tan,<sup>†</sup> Antons Sizovs,<sup>†</sup> Ninghui Cheng,<sup>§</sup> Meng C. Wang<sup>¶</sup> and Jin Wang<sup>\*†§</sup>

*<sup>†</sup>Department of Pharmacology, <sup>¶</sup>Department of Molecular and Human Genetics and Huffington Center on Aging, <sup>‡</sup>Integrative Molecular and Biomedical Sciences Graduate Program, <sup>§</sup>USDA/ARS Children Nutrition Research Center and Department of Pediatrics, <sup>§</sup>Center for Drug Discovery, Dan L. Duncan Cancer Center, and Cardiovascular Research Institute, Baylor College of Medicine, Houston, TX 77030.*

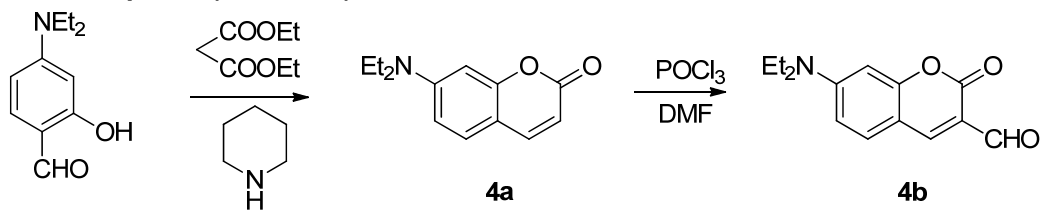
Corresponding author email: [wangji@bcm.edu](mailto:wangji@bcm.edu)

## Table of Contents

Chemical synthesis and characterization .....	S3
Ratiometric quantification equations.....	S6
Analysis of TQ Green Intracellular Distribution and Accuracy of GSH Quantification .....	S7
Example of image processing and statistical analysis.....	S8
Influence of instrument on fluorescence measurement and ratiometric quantitation.....	S9
Table S1. Summary of structures of tested GSH probes.....	S10
Table S2. Summary of quantum yields of GSH probes .....	S11
Figure S1. GSH stability in air.....	S12
Figure S2. Calibration curves for TQ Green .....	S13
Figure S3. Simulation of signal changes with different $K_d$ values .....	S14
Figure S4. Confocal images of TQ Green and TQ Green-AM on cells.....	S15
Figure S5. Confocal images of TQ Green on polystyrene beads .....	S16
Figure S6. Calibration curve for confocal microscope .....	S17
Figure S7. Fluorescent spectra of TQ Green and TQ Green-GSH.....	S18
Figure S8. Reaction kinetics of TQ Green and compound 3a .....	S19
Figure S9. $^1\text{H-NMR}$ (400 MHz, $\text{CD}_3\text{OD}$ ) spectrum of compound 3a.....	S20
Figure S10. $^1\text{H-NMR}$ (400 MHz, $\text{CD}_3\text{OD}$ ) spectrum of TQ Green.....	S21
Figure S11. $^1\text{H-NMR}$ (400 MHz, $\text{CDCl}_3$ ) spectrum of TQ Green-AM.....	S22
Figure S12. $^{13}\text{C-NMR}$ (100 MHz, $\text{CDCl}_3$ ) spectrum of TQ Green-AM.....	S23

## Chemical synthesis and characterization:

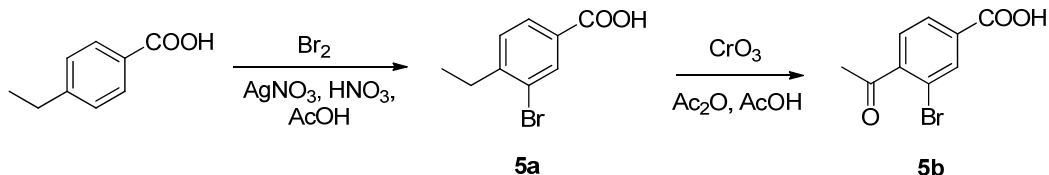
### Synthesis of Fluorophore (Module A)



Compounds **4a** and **4b** were synthesized according to literature.<sup>S1</sup> Briefly, 4-diethylaminosalicylaldehyde (1.93 g, 10 mmol), diethylmalonate (3.2 g, 20 mmol) and piperidine (1.0 mL) were mixed in absolute ethanol (30 mL) and refluxed for 18 hours. All volatiles were evaporated under reduced pressure, then a mixture of concentrated HCl (20 mL) and acetic acid (20 mL) was added. Reaction mixture was stirred at 115 °C for 19 hours. The solution was cooled to room temperature and poured into 100 mL of ice water. Upon using NaOH solution (40%) to adjust pH to 5, brown precipitate formed immediately. After stirring for 1 hour and cooling to 4 °C, the mixture was filtered, washed with water, and then dried to give the desired product 7-diethylaminocoumarin **4a** (2.06 g, 95%).

Anhydrous DMF (6.5 mL) was added dropwise to POCl<sub>3</sub> (6.5 mL) at 60 °C under N<sub>2</sub> atmosphere and stirred for 30 minutes to yield a red solution. The mixture was added to a solution of 7-diethylaminocoumarin **4a** (4.50 g, 20.7 mmol) in DMF (30 mL) to allow a scarlet suspension. The mixture was stirred at 70 °C for 16 hours and then poured into 300 mL of ice water. Upon addition of NaOH (40%) solution to adjust pH to 5, an large amount of precipitate appeared. The crude product was filtered, thoroughly washed with water, dried and recrystallized in absolute ethanol to give the desired compound **4b** (3.0 g, 58%). <sup>1</sup>H-NMR in DMSO-d<sub>6</sub> was performed for both compounds and matched reference results.<sup>S1</sup>

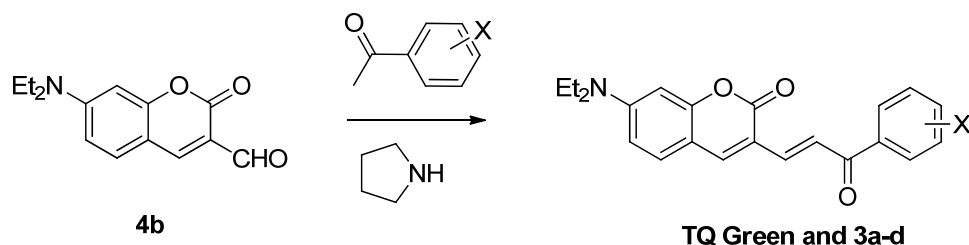
### Synthesis of Function Ketone (Module C)



Compounds **5a** and **5b** were synthesized according to literature.<sup>S2</sup> Briefly, bromine (0.7 mL, 14 mmol) was added to a solution of 4-ethylbenzoic acid (1.5 g, 10 mmol) in acetic acid (30 mL), nitric acid (6.5 mL) and water (5 mL). A solution of silver nitrate (1.7 g, 10 mmol) in water was added dropwise with vigorous stirring. The reaction mixture was stirred overnight at room temperature with a large amount of yellow precipitation. Resulting solution was filtrated and all volatile was removed under reduced pressure to yield the crude product as white powder, which was recrystallized in ethyl acetate and hexane to give 3-bromo-4-ethylbenzoic acid **5a** (0.9 g, 40%).

Chromium (VI) oxide (2.42 g, 2.42 mmol) was dissolved in a mixture of acetic acid (10 mL) and acetic anhydride (7 mL). A solution of 3-bromo-4-ethylbenzoic acid **5a** (1.03 g, 4.52 mmol) in acetic acid (15 mL) was added dropwise. During addition, 3-bromo-4-ethylbenzoic acid **5a** partially crushed out. An additional acetic acid (10 mL) was used to rinse **5a** and combined with the reaction mixture. The reaction mixture was stirred overnight under nitrogen at room temperature. After addition of water (100 mL), the mixture was extracted with diethyl ether. The collected organic layer was washed with water and then evaporated to give crude product as a white powder, which was then recrystallized in ethyl acetate and hexane to afford 4-acetyl-3-bromobenzoic acid **5b** (0.81 g, 74%). <sup>1</sup>H-NMR in CDCl<sub>3</sub> were performed for both compounds and matched with the literature results.<sup>S2</sup>

### Synthesis of Michael Acceptor (Module B)

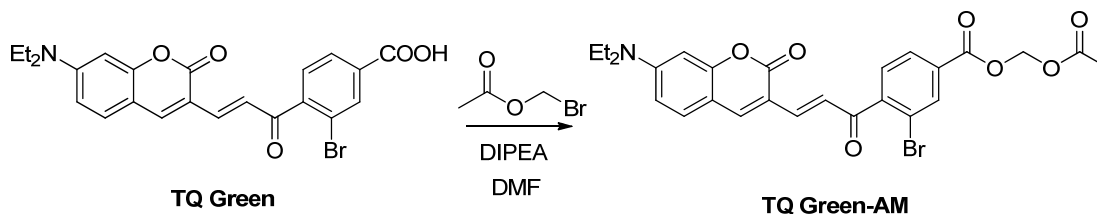


To a solution of **4b** (123 mg, 0.500 mmol) and different ketones (1.8 equiv, Table S1) in CH<sub>2</sub>Cl<sub>2</sub>/EtOH (1:1, v/v, 4 mL) was added 2 drops of pyrrolidine. The resulting solution (usually red) was stirred at r.t. for additional 12 h to afford a scarlet solution. All solvent was removed under vacuum. The crude product was then purified by reverse phase chromatography (C18 column, elute with ACN in water 5-40%). Then, recrystallization was performed in ethanol to further purify compounds **3a** and **TQ Green**.

Compound **3a**: <sup>1</sup>H-NMR (400 MHz, CD<sub>3</sub>OD): δ 8.20 (s, 1H), 8.13-7.98 (m, 5H), 7.72 (d, *J* = 15.6 Hz, 1H), 7.49 (d, *J* = 9.2 Hz, 1H), 6.78 (dd, *J* = 2.4, 9.2 Hz, 1H), 6.56 (d, *J* = 2.4 Hz, 1H), 3.51 (dd, *J* = 7.2, 14.2 Hz, 4H), 1.23 (t, *J* = 6.8 Hz, 6H); ESI-MS (*m/z*): [M + H]<sup>+</sup> calculated for C<sub>23</sub>H<sub>21</sub>NO<sub>5</sub>, 392.1; found, 392.0.

**TQ Green**: <sup>1</sup>H-NMR (400 MHz, CD<sub>3</sub>OD): δ 8.22 (d, *J* = 1.2 Hz, 1H), 8.06 (s, 1H), 7.98 (dd, *J* = 1.2, 7.8 Hz, 1H), 7.49-7.26 (m, 4H), 6.75 (dd, *J* = 2.8, 9 Hz, 1H), 6.53 (d, *J* = 2.4 Hz, 1H), 3.51 (dd, *J* = 7.2, 14.2 Hz, 4H), 1.21 (t, *J* = 6.8 Hz, 6H); ESI-MS (*m/z*): [M + H]<sup>+</sup> and [M+2 + H]<sup>+</sup> calculated for C<sub>23</sub>H<sub>20</sub>BrNO<sub>5</sub>, 470.1 and 472.1; found, 469.9 and 471.9.

### Synthesis of Cell Permeable GSH Probe



To a TQ Green (5.0 mg, 0.010 mmol) solution in anhydrous DMF (1 mL) were added bromomethyl acetate (0.0062 mL, 0.053 mmol) and DIPEA (0.0075 mL, 0.042 mmol) under nitrogen protection. The reaction mixture was allowed to stir at room temperature overnight, and then concentrated under reduced pressure. The residue was purified by flash column chromatography (elute with hexane in ethyl acetate 20-50%) to afford TQ Green-AM as an orange solid. (4.0 mg, 69%).

**TQ Green-AM**: <sup>1</sup>H-NMR (400 MHz, CDCl<sub>3</sub>): δ 8.30 (d, *J* = 2.0 Hz, 1H), 8.06 (dd, *J* = 2.0, 8.0 Hz, 1H), 7.77 (s, 1H), 7.54-7.29 (m, 4H), 6.60 (dd, *J* = 2.0, 8.0 Hz, 1H), 6.47 (d, *J* = 2.0 Hz, 1H), 6.00 (s, 2H), 3.44 (dd, *J* = 8.0, 16.0 Hz, 4H), 2.15 (s, 3H), 1.23 (t, *J* = 6.8 Hz, 6H); <sup>13</sup>C-NMR (100 MHz, CDCl<sub>3</sub>): δ 194.02, 169.55, 163.45, 160.04, 156.92, 152.25, 146.15, 145.53, 142.18, 134.74, 131.33, 130.27, 128.93, 126.79, 125.64, 119.58, 114.10, 109.67, 108.81, 96.95, 45.09, 29.67, 20.73, 12.45; ESI-MS (*m/z*): [M + H]<sup>+</sup> and [M+2 + H]<sup>+</sup> calculated for C<sub>26</sub>H<sub>24</sub>BrNO<sub>7</sub>, 541.1 and 543.1, found, 540.9 and 542.9.

### Determination of Compounds 3a-d and TQ Green Reactivity against Thiols

Compounds **3b-d** were dissolved in DMSO (10 mM) and 1 eq of 2 M β-mercaptoethanol (BME) was added. Compounds **3a** and TQ Green were dissolved in PBS buffer (10 mM, pH 7.4) with 1% DMSO. GSH solution was added to reach a final concentration of 80 mM with compound **3a** at 10 μM and TQ Green at 16 μM, respectively. All solutions were then monitored continuously with UV-Vis and fluorimeter for 2 h (Table S1).

### Determination of Reaction Kinetics of TQ Green with GSH

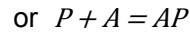
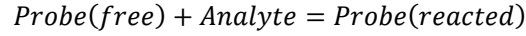
GSH in PBS was added to a solution of TQ Green in PBS buffer (10 mM, pH 7.4) containing 1 % DMSO. The final concentrations of GSH and TQ Green were 10 mM and 16 μM, respectively. The solutions were then monitored continuously with UV-Vis spectrometer (Figure S8).

## REFERENCE

- S1. Tae-Ki Kim; Dong-Nam Lee; Hae-Jo Kim, *Tetrahedron Letters*, **2008**, 49, 4879.  
S2. Van Rompaey, Philippe et al, *PCT Int. Appl.*, 2007042321, **2007**

## Deduction of Ratiometric Quantification

The reversible reaction equation is:



According to the reaction equation, the dissociation constant is:

$$K_d = \frac{[P][A]}{[AP]}$$

$[P]$  and  $[AP]$  are the concentrations of free and reacted probes, respectively.

Absorptions at two peak wavelengths are:

$$A_{\lambda_1} = \varepsilon_{P,\lambda_1}[P] + \varepsilon_{AP,\lambda_1}[AP]$$

$$A_{\lambda_2} = \varepsilon_{P,\lambda_2}[P] + \varepsilon_{AP,\lambda_2}[AP]$$

$\varepsilon$  is the molar absorption coefficient, Subscripts  $P$  and  $AP$  stands for free and reacted probes, respectively.

The ratio can be deduced as:

$$R = \frac{A_{\lambda_1}}{A_{\lambda_2}} = \frac{\varepsilon_{P,\lambda_1}[P] + \varepsilon_{AP,\lambda_1}[AP]}{\varepsilon_{P,\lambda_2}[P] + \varepsilon_{AP,\lambda_2}[AP]}$$

From dissociation constant, we can substitute all  $[P]$  with  $[AP]$ :

$$[AP] = [P][A]/K_d$$

$$R = \frac{\varepsilon_{P,\lambda_1} + \frac{\varepsilon_{AP,\lambda_1}}{K_d}[A]}{\varepsilon_{P,\lambda_2} + \frac{\varepsilon_{AP,\lambda_2}}{K_d}[A]}$$

So, the absorption ratio should fit in the following equation, which is not linear to the analyte concentration:

$$R = \frac{\varepsilon_{P,\lambda_1}}{\varepsilon_{P,\lambda_2}} + \frac{\varepsilon_{AP,\lambda_1} - \frac{\varepsilon_{AP,\lambda_1}}{\varepsilon_{AP,\lambda_2}}\varepsilon_{P,\lambda_2}}{\varepsilon_{P,\lambda_2} + \frac{\varepsilon_{AP,\lambda_2}}{K_d}[A]} = P + \frac{Q}{S + T[A]}$$

The equation can be reduced to linear when  $\varepsilon_{AP,\lambda_2} = 0$  or  $K_d$  is much larger than the analyte concentration.

Otherwise, the analyte concentration and  $R$  follows the relationship below:

$$[A] = K_d \left( \frac{R - \left( \frac{\varepsilon_{P,\lambda_1}}{\varepsilon_{P,\lambda_2}} \right)}{\left( \frac{\varepsilon_{AP,\lambda_1}}{\varepsilon_{AP,\lambda_2}} \right) - R} \right) \left( \frac{\varepsilon_{P,\lambda_2}}{\varepsilon_{AP,\lambda_2}} \right)$$

When there is no analyte present, only pure probe contributes to the absorbance:

$$A_{\lambda_1} = \varepsilon_{P,\lambda_1}[P]$$

$$A_{\lambda_2} = \varepsilon_{P,\lambda_2}[P]$$

$$R = \frac{\varepsilon_{P,\lambda_1}[P]}{\varepsilon_{P,\lambda_2}[P]} = \frac{\varepsilon_{P,\lambda_1}}{\varepsilon_{P,\lambda_2}} = R_{min}$$

When all the probe is saturated by analyte, only bounded probe contributes to the absorbance:

$$A_{\lambda_1} = \varepsilon_{AP,\lambda_1}[AP]$$

$$A_{\lambda_2} = \varepsilon_{AP,\lambda_2}[AP]$$

$$R = \frac{\varepsilon_{AP,\lambda_1}[AP]}{\varepsilon_{AP,\lambda_2}[AP]} = \frac{\varepsilon_{AP,\lambda_1}}{\varepsilon_{AP,\lambda_2}} = R_{max}$$

Combined all above together:

$$[A] = K_d \left( \frac{R - R_{min}}{R_{max} - R} \right) \left( \frac{\varepsilon_{P,\lambda_2}}{\varepsilon_{AP,\lambda_2}} \right)$$

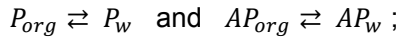
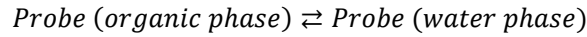
$$[A] = K_d' \frac{R - R_{min}}{R_{max} - R}$$

Specific to TQ Green,  $\lambda_1 = 405$  nm, and  $\lambda_2 = 488$  nm.

### Analysis of TQ Green Intracellular Distribution and Accuracy of GSH Quantification

The following analysis is based on two assumptions: (1) TQ Green only distributes in cytosol and in lipids that are in contact with cytosol; (2) the cytosolic GSH is evenly distributed.

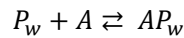
Assuming the distribution of cytosolic TQ Green reaches equilibrium, the distribution equilibrium is:



$$\text{Therefore, } K_P = \frac{P_{org}}{P_w} \quad \text{and} \quad K_{AP} = \frac{AP_{org}}{AP_w},$$

where  $K_P$  and  $K_{AP}$  are distribution coefficients of P and AP, respectively.

Because analyte (GSH) is only present in water phase in this case, so the coupled equilibrium is:



$$K_d = \frac{[P_w][A]}{[AP_w]}$$

To simplify the analysis, we assume that the spectra of AP and P does not overlap at all, then the fluorescent intensity at two channels are:

$$\begin{aligned} I_P &= \varepsilon_{P,w}[P_w] + \varepsilon_{P,org}[P_{org}] = \varepsilon_{P,w}[P_w] + \varepsilon_{P,org}K_P[P_w] \\ &= (\varepsilon_{P,w} + \varepsilon_{P,org}K_P)[P_w] = \varepsilon_P'[P_w] \end{aligned}$$

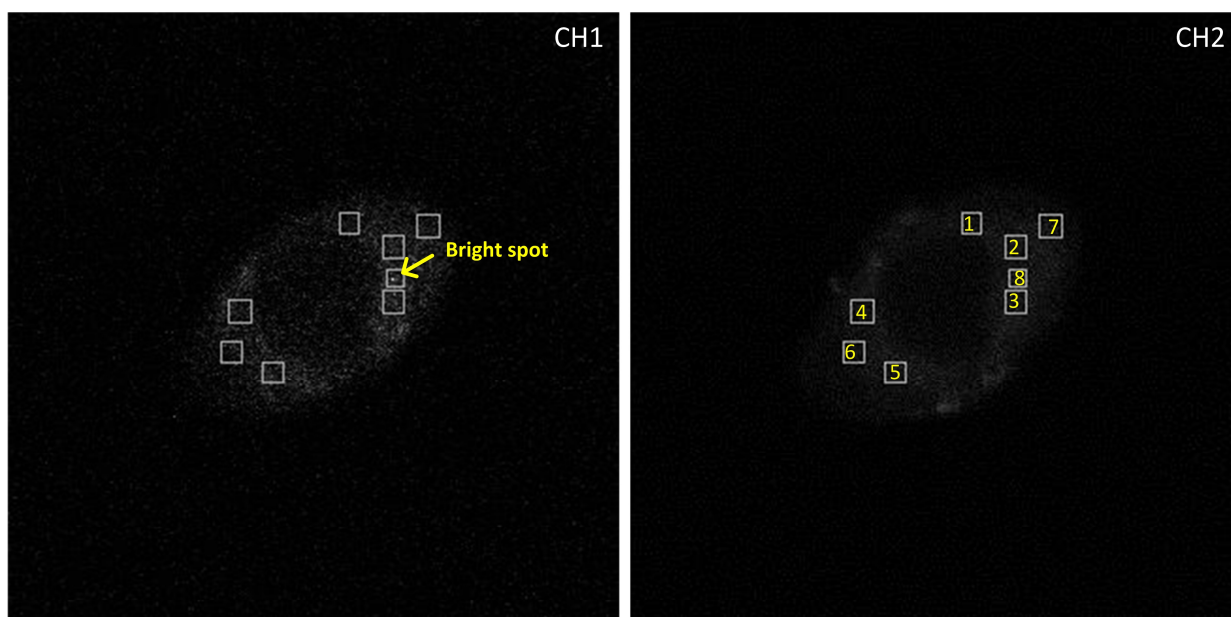
$$\begin{aligned} I_{AP} &= \varepsilon_{AP,w}[AP_w] + \varepsilon_{AP,org}[AP_{org}] = \varepsilon_{AP,w}[AP_w] + \varepsilon_{AP,org}K_{AP}[AP_w] \\ &= (\varepsilon_{AP,w} + \varepsilon_{AP,org}K_{AP})[AP_w] = \varepsilon_{AP}''[AP_w] \end{aligned}$$

Therefore, the analyte concentration can be derived as:

$$[A] = K_d \frac{[AP_w]}{[P_w]} = K_d \frac{I_{AP}/\varepsilon_{AP}''}{I_P/\varepsilon_P'} = K_d'' \frac{I_{AP}}{I_P}$$

While the  $K_d''$  may not be the same in different environments, the analyte concentration [A] is proportional to the fluorescence intensity ratio of AP and P.

## Example of Image Processing and Statistical Analysis



Summary table of measurements from the example cell

Location	Area	Channel 1 ( $\lambda_{ex}=405$ nm)			Channel 2 ( $\lambda_{ex}=488$ nm)			Ratio of CH1/CH2
		Average	Min	Max	Average	Min	Max	
Background	NA	177.382	148	573	172.086	153	240	NA
1	2.643	448.100	163	931	397.218	200	629	1.205
2	3.171	624.341	174	1798	505.447	312	760	1.343
3	3.171	674.758	190	2423	508.545	275	865	1.480
4	3.460	502.007	168	1454	447.910	227	689	1.179
5	2.907	603.198	160	1589	485.702	283	787	1.360
6	2.907	454.380	156	1857	378.107	186	817	1.347
7	3.460	476.806	153	1347	417.312	210	748	1.223
8 (excluded)	1.946	749.309	209	4095	512.259	306	795	1.683
Ratio average of the example cell:					1.305 ± 0.107			

As shown above, a typical image acquired from a confocal microscope contains intensity information from two fluorescent channels. For each cell, the average intensities of the two channels from at least five randomly chosen areas (squares in our case) within the cytosol (nucleus was excluded) were measured. It should be noted that for each matched pair of average intensity values, the data must be measured at the exact same location for reasonable results because the absolute intensities can vary a lot throughout the cell due to probe distribution and heterogeneity within the cell. The ratio was then calculated after subtracting background fluorescence. Bright spots/oversaturated pixels were excluded from statistical analysis based on the dynamic range of the CCD camera (0-4095), as illustrated above at location 8. For each sample, we analyzed the statistical average ratio from at least 30 cells in the confocal images, including the standard curve measured with polystyrene beads (see below, Figure S5, S6). It should be noted that with the settings of our confocal microscope, we found that  $R$  is in a reasonable linear relationship with GSH concentrations. This is because  $K_d'$  is an instrument dependent parameter and  $R$  is proportional to GSH concentrations if  $K_d'$  is much larger than 10 mM (refer to SI for details). Therefore, for all the cell imaging studies,  $R$ , which is CH1/CH2 in this case, is plotted against GSH concentrations in standard curves and quantification, instead of  $(R-R_{min})/(R_{max}-R)$ .



## Influence of Instrument on Fluorescence Measurement and Ratiometric Quantitation

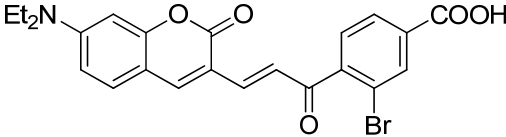
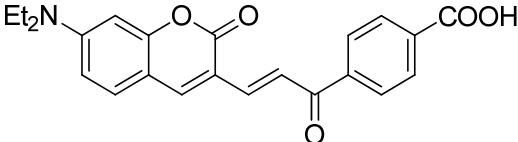
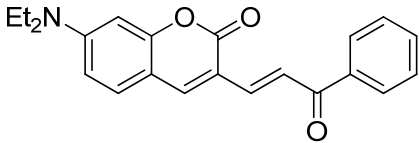
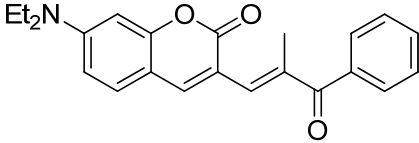
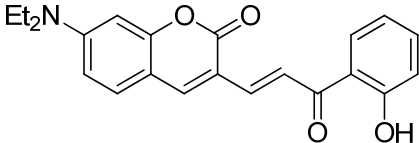
Fluorescence measurement is instrument dependent. Higher energy of the excitation light source can result in higher emission signals. Because the energy distribution at certain wavelength is different for different light sources, different fluorimeters may exhibit difference in measurements. For the same token, the wavelength dependent sensitivity of fluorimeter detectors also contributes to the instrument dependency of fluorescence measurement (refer to *Anal. Chem.* **2010**, *82*, 2129–2133 for detailed discussion).

A general misconception in ratiometric quantitation is that ratiometric probes can not only quantify analyte concentrations independent of the probe concentration but also eliminate all other variables, including instrument dependency. However, this notion is wrong for fluorescence measurements, especially in confocal microscope measurements. Because fluorescent intensity is dependent on the energy of the excitation laser beam and the detector responses at different wavelengths, ratiometric measurements are indeed affected by illumination power and detector sensitivity, and thus instrument dependent. In fact, with the same dye solution, different ratios can be obtained based on different instrumental settings. For example, if a hypothetical dye solution X is excited at two wavelengths with different energies, the following data is what one will expect:

$\lambda_{ex}$	Instrument Setting 1		Instrument Setting 2		Instrument Setting 3	
	Excitation Power	Emission Intensity	Excitation Power	Emission Intensity	Excitation Power	Emission Intensity
$\lambda_1$	100	50	50	25	100	50
$\lambda_2$	100	25	100	25	50	12.5
Em Ratio of $\lambda_1/\lambda_2$	<b>2</b>		<b>1</b>		<b>4</b>	

As shown in the table above, different ratios can be obtained by manipulating the energy of the excitation laser. As a matter of fact, we observed similar results in our own experiments. Therefore, to perform a reliable quantitation, all the calibration and measurements should be done on the same day with the same instrument and the same settings throughout the experiment.

Table S1.

Structure	Solubility	$K_d'$ <sup>***</sup>
 <p style="text-align: center;"><b>3</b> ThiolQuant Green (TQ Green)</p>	Water *	14.8 mM
 <p style="text-align: center;"><b>3a</b></p>	Water *	1.5 mM
 <p style="text-align: center;"><b>3b</b></p>	DMSO **	N/A
 <p style="text-align: center;"><b>3c</b></p>	DMSO **	N/A
 <p style="text-align: center;"><b>3d</b></p>	DMSO **	~2 mM

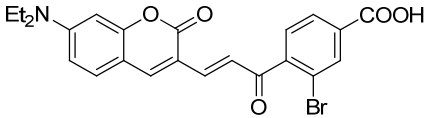
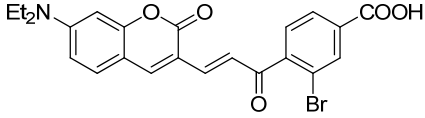
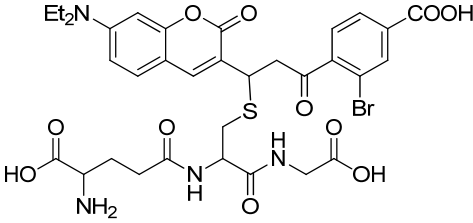
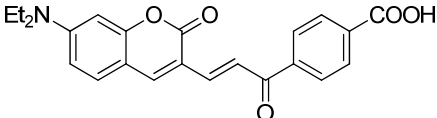
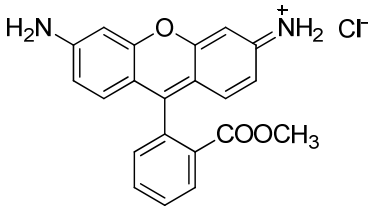
\* Solubility in PBS buffer > 0.5 mM

\*\* Solubility in PBS buffer < 10  $\mu$ M

\*\*\* Observed dissociation constant ( $K_d'$ ) was determined by reaction with various concentration of GSH in water and  $\beta$ -mercaptoethanol in DMSO

A series of GSH probes were synthesized (Table S1) following the parental structure **3b** (protected 7-Amino coumarin conjugates with phenyl Michael acceptor). The presence of an electron-donating group, such as a methyl group (compound **3c**), on module B significantly blocks the Michael addition between thiol and probe. In contrast, decreasing electron density on module B through electron-withdrawing groups on module C (compound **3a** and TQ Green) or intramolecular hydrogen bonding (compound **3d**), favors the sensing reaction. To facilitate applications *in vitro*, we chose carboxylic acid as substitutes on module C, because 1) it greatly improves the water solubility of the whole molecule; and 2) it can be modified through esterification to enhance cell permeability. After several iterations, we found that introduction of bromine to module C (TQ Green) can produce a GSH probe with an appropriate equilibrium constant.

Table S2.

Structure	Solvent	Quantum Yield
 <p><b>3 - TQ Green</b></p>	Methanol	0.16±0.05
 <p><b>3 - TQ Green</b></p>	PBS	0.0094±0.0004
 <p><b>TQ Green-GSH</b></p>	PBS	0.0059±0.0003
 <p><b>3a</b></p>	Methanol	0.062±0.002
 <p><b>Rhodamine 123</b></p>	Methanol	0.94*

\*Used as standard

Quantum yields of synthesized GSH probes and a GSH adduct with Rhodamine 123 as the standard. Quantum yields were determined using a comparative method described by Williams *et al.*<sup>S3</sup> The bromine atom on phenyl ring potentially enhances the push-pull effect of the coumarin-based fluorophore, thus increases the quantum yield.

S3. A. T. R. Williams, S. A. Winfield and J. N. Miller, Relative fluorescence quantum yields using a computer controlled luminescence spectrometer, *Analyst*, 1983, **108**, 1067.

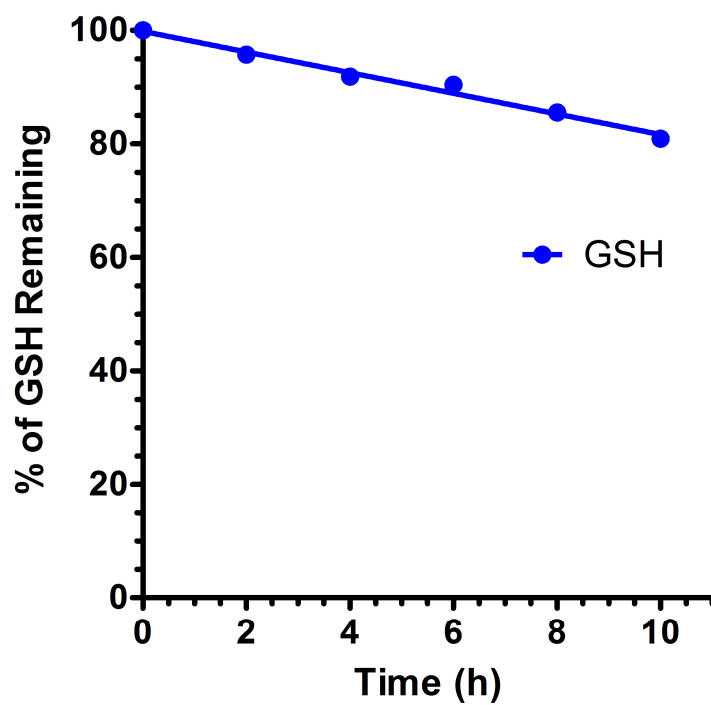


**Figure S1.** GSH stability in air. GSH solution (10 mM) was placed in a capped Eppendorf tube. Samples of solution were taken out for HPLC measurement every two hours. About 20% of GSH was oxidized over 10 h time period. Percentage was calculated from the HPLC peak area monitored at 254 nm.

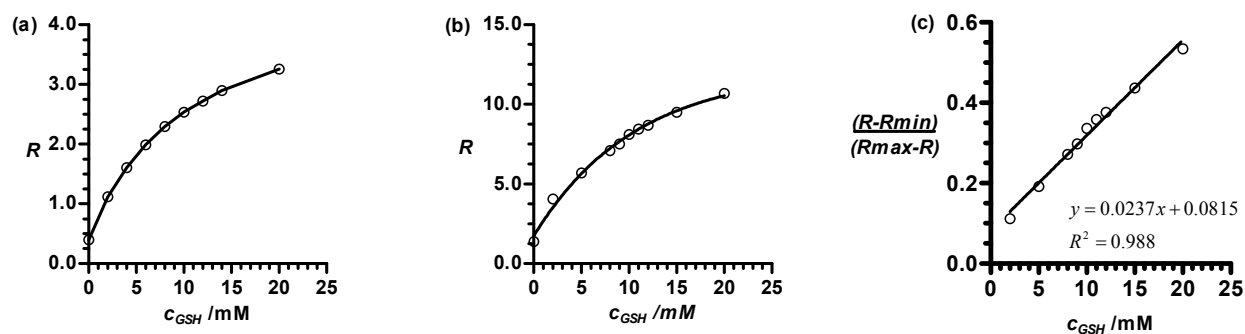


**Figure S2.** Calibration curves for TQ Green. (a) Ratio  $R$  derived from absorption plotted against GSH concentration,  $R$  stands for the ratio of absorption signals between 405 and 488 nm; (b) Ratio  $R$  derived from fluorescence plotted against GSH concentration; (c) The linear relationship between  $(R-R_{\text{min}})/(R_{\text{max}}-R)$  and GSH concentration based on fluorescence measurement. Fluorescent ratio  $R$  stands for ratio of signals between 468 nm ( $\lambda_{\text{ex}} = 405 \text{ nm}$ ) and 592 nm ( $\lambda_{\text{ex}} = 488 \text{ nm}$ ). It should be noted that some previous studies plotted  $R$  directly against analyte concentration to afford a linear relationship. It should be cautioned that this type of linear relationship is valid only when 1) there is no spectral overlap between the absorption and/or emission bands from probe and probe-analyte adduct or 2) the dissociation constant is much larger (preferably 100 times larger) than the analyte concentration. In our study, because the spectral overlap at the two monitoring wavelengths occurs, plotting  $R$  against GSH concentration confers a non-linear relationship.

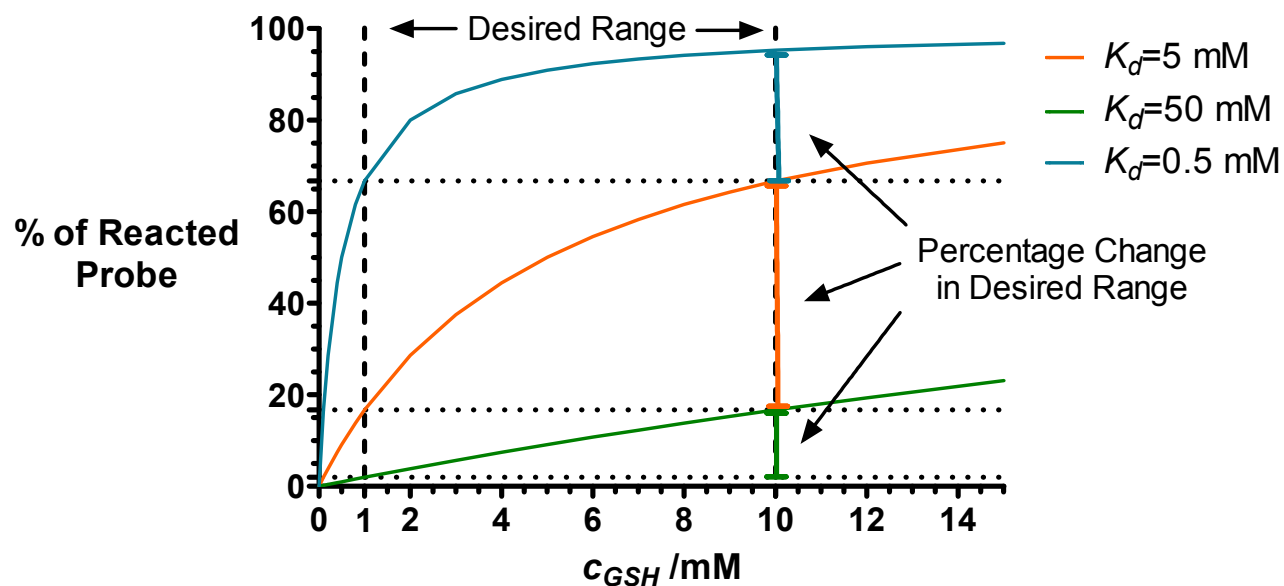


**Figure S3.** Simulation of signal changes with different  $K_d$  values. Proper  $K_d$  value results in the largest signal change, allowing more accurate measurements. Using GSH as an example, if the expected range of GSH concentration is 1-10 mM, the optimal  $K_d$  would be ~3 mM (orange curve). Deviations from this  $K_d$  will result in weakened response to the concentration changes (blue and green curves). Additionally, the apparent dissociation constant  $K_d'$  also depends on the relative signal intensities from the free and reacted probes.

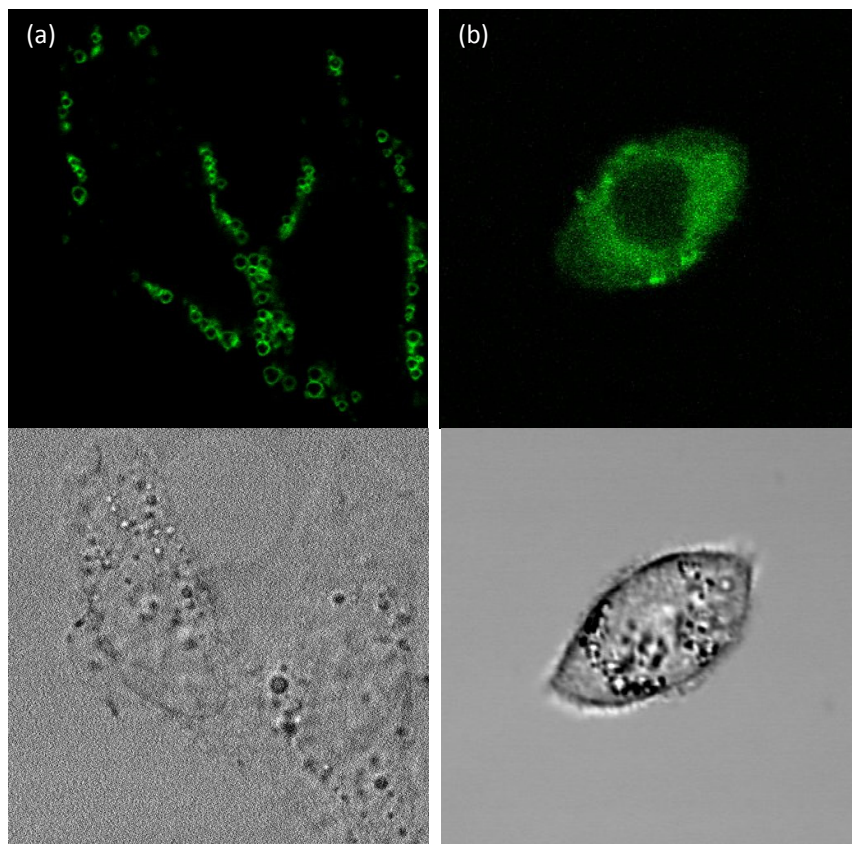


**Figure S4.** Confocal images at 488 nm channel of **(a)** TQ Green (acid form), **(b)** TQ Green-AM (ester form) interacting with cells. Most of the acid form probe molecules were trapped in the membrane, but AM-ester form was able to penetrate through cell membrane and stays in cytosol after hydrolysis.

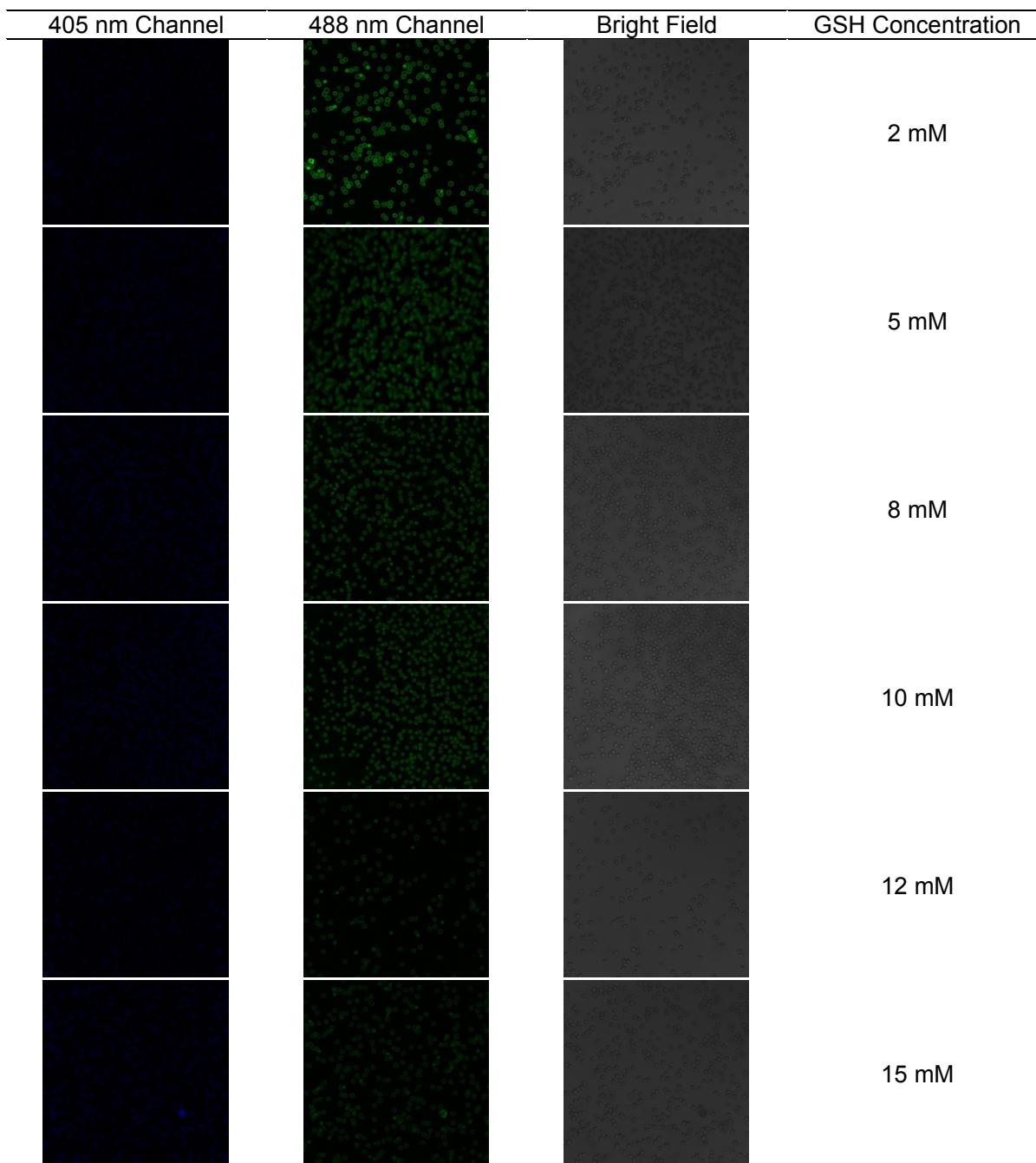


**Figure S5.** Confocal fluorescent images of TQ Green adsorbed on polystyrene beads in various concentrations of GSH solution. These images were used for calibration of confocal microscope because we encountered a technical difficulty that confocal microscopes are unable to measure the fluorescence intensity of a homogenous solution due to lack of a focal point. To solve this problem, we physically adsorbed TQ Green to the surface of 4.5  $\mu\text{m}$  polystyrene beads, which allowed us to quantify the fluorescence intensity ratio with excitation at 405 and 488 nm in different concentrations of GSH solution.



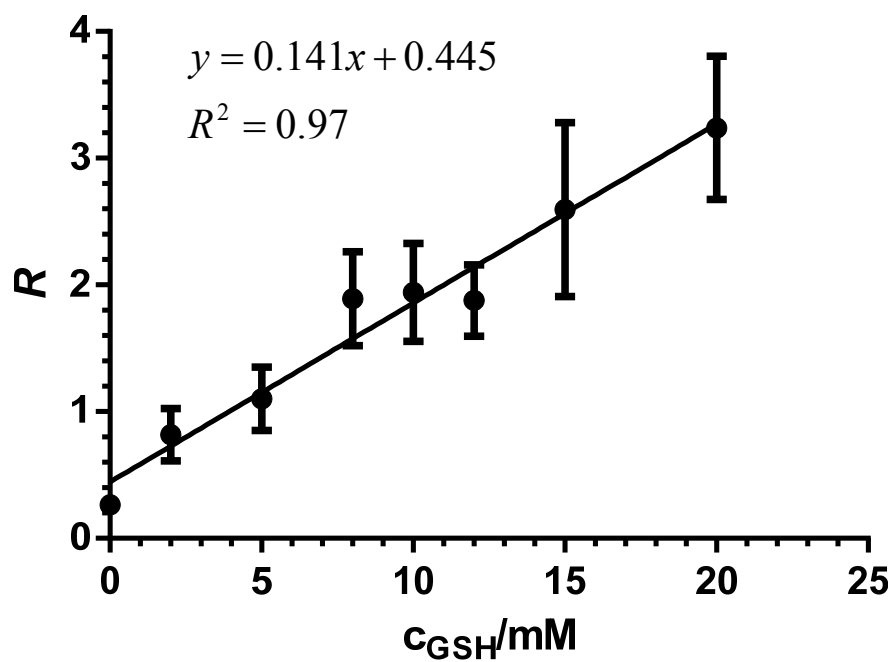


**Figure S6.** Calibration curve for confocal microscope based on fluorescent images from Figure S5. Intensity average from both channels (405 nm and 488 nm excitation) was used for calculation, detailed image processing was described above on page S8.

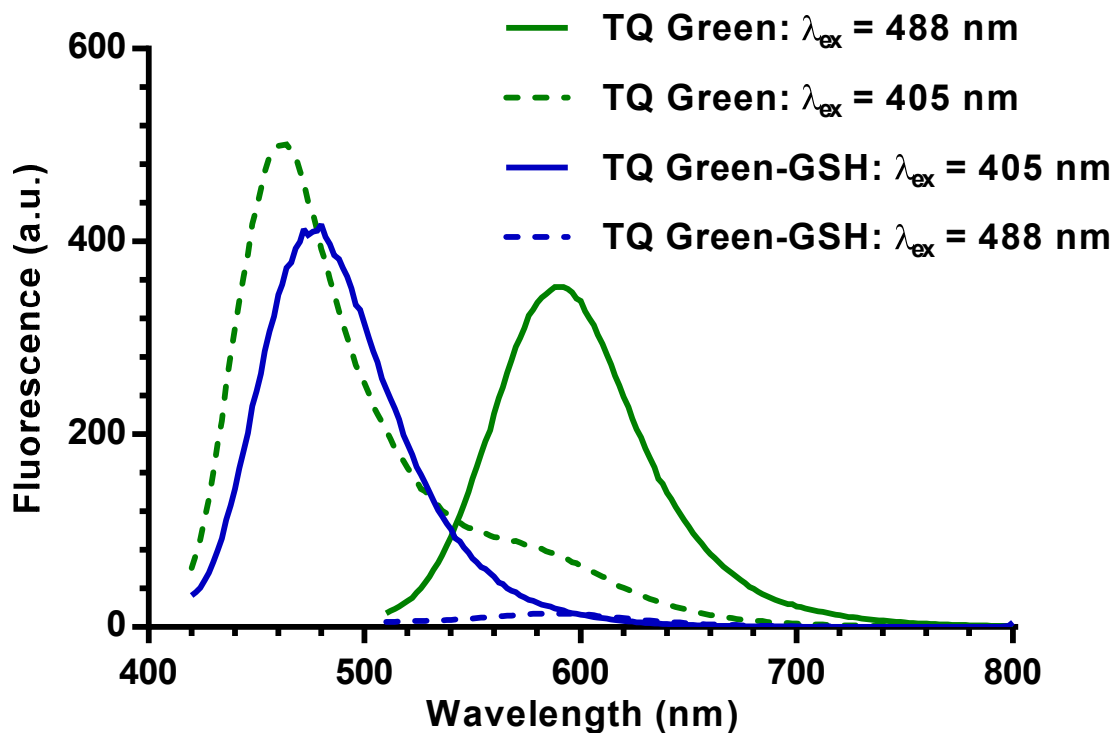


**Figure S7.** Fluorescent spectra of TQ Green and TQ Green-GSH with excitation wavelength at 405 nm and 488 nm. The fluorescent signal with 405 nm excitation does not have significant changes upon addition of GSH, due to the coincidence that the loss of TQ Green fluorescence is compensated by the gain of TQ Green-GSH fluorescence. The fluorescent signal with 488 nm excitation changes dramatically, so that the ratio between the signals from two channels changes significantly as well.

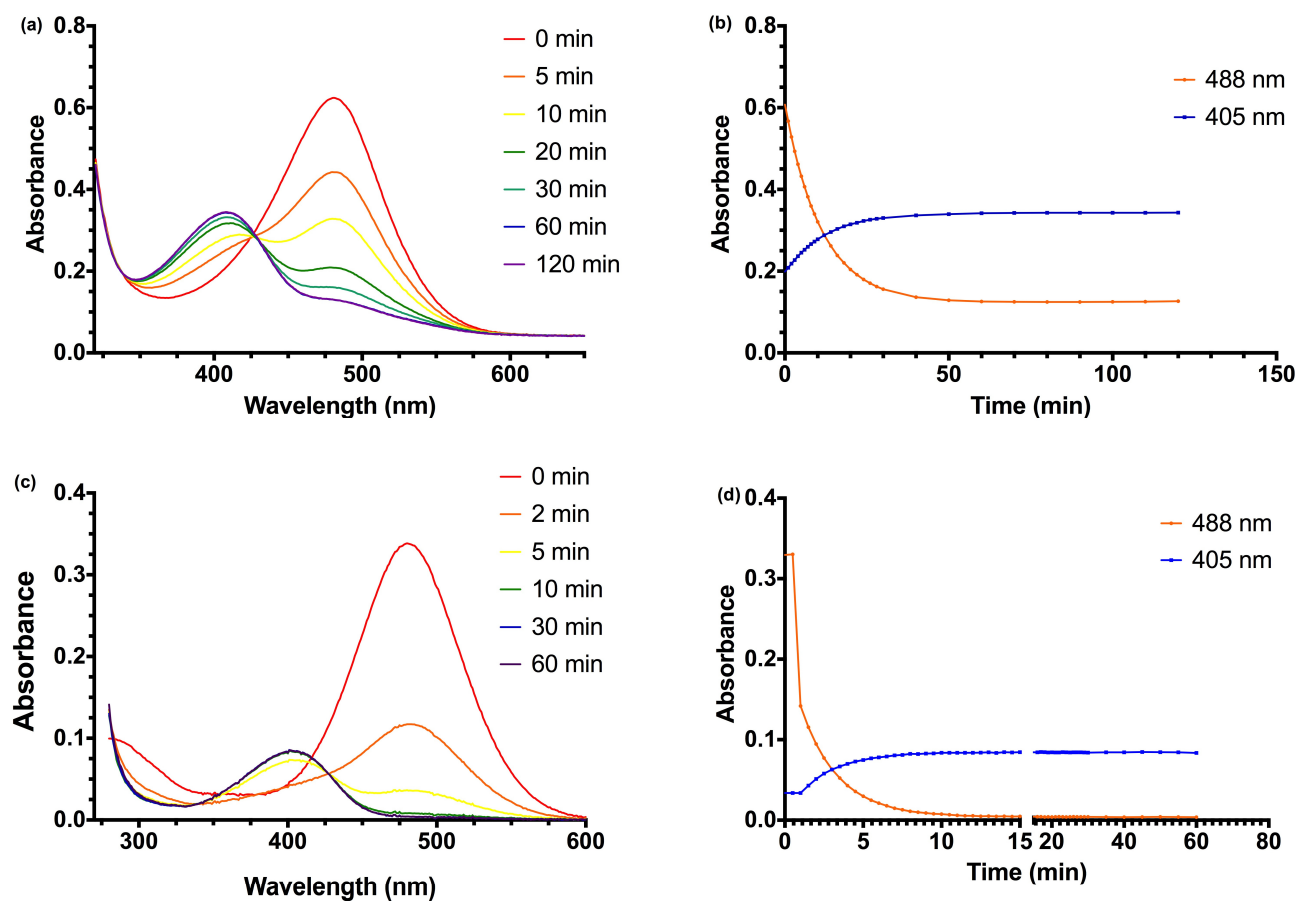


**Figure S8.** (a,b) Reaction kinetics of TQ Green. Time-dependent spectra and kinetics were shown for TQ Green (16  $\mu$ M) reacting with 10mM of GSH in PBS. At room temperature, the reaction takes  $\sim$ 30 minutes to reach 95% of conversion. (c,d) Reaction kinetics of probe **3a**. Time-dependent spectra and kinetics were shown for probe **3a** (10  $\mu$ M) reacting with 10mM of GSH in PBS. At room temperature, the reaction takes  $\sim$ 6 minutes to reach 95% of conversion.

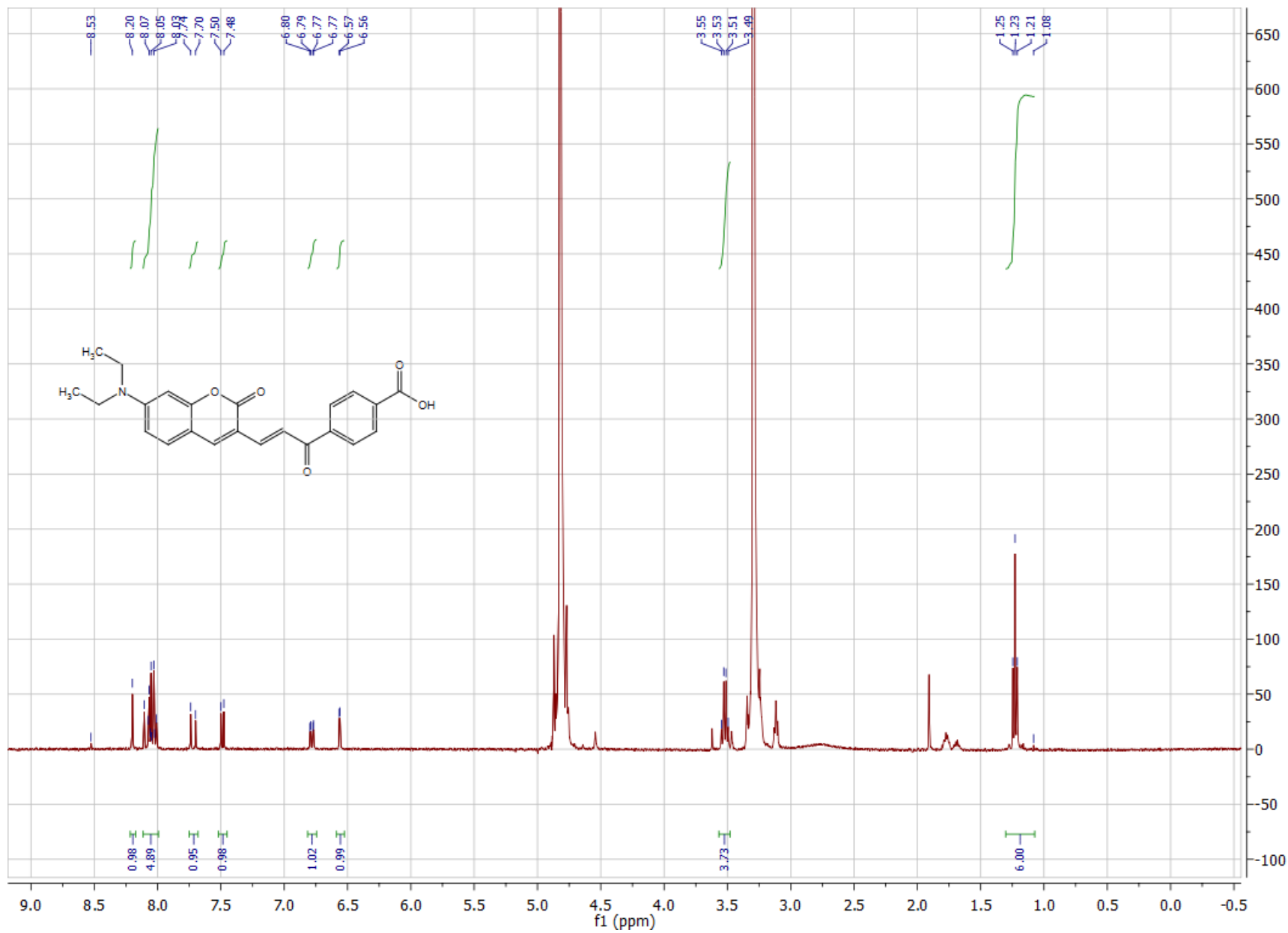
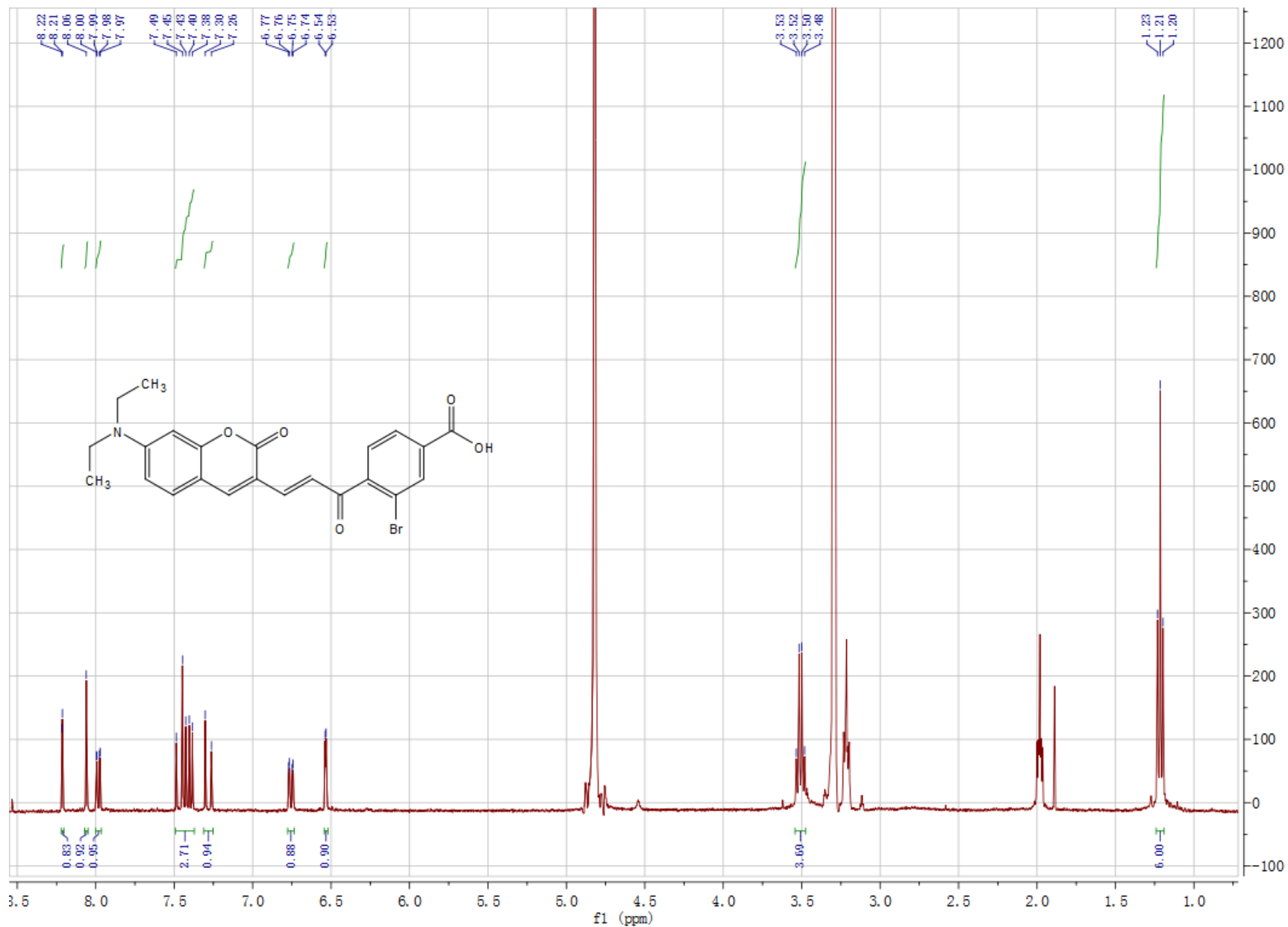


Figure S9. <sup>1</sup>H-NMR (400 MHz, CD<sub>3</sub>OD) spectrum of compound 3a.



**Figure S10.** <sup>1</sup>H-NMR (400 MHz, CD<sub>3</sub>OD) spectrum of ThiolQuant Green.

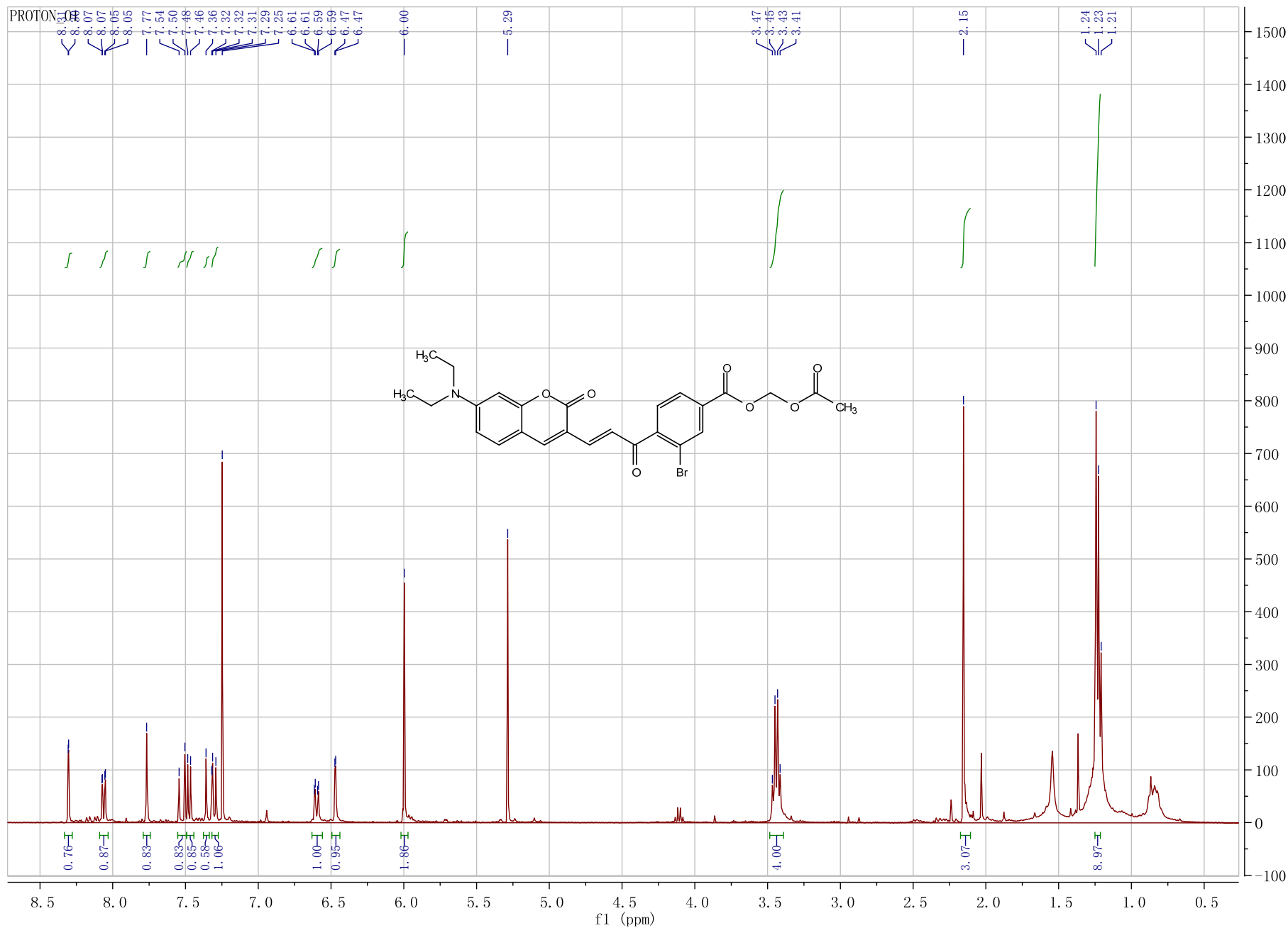
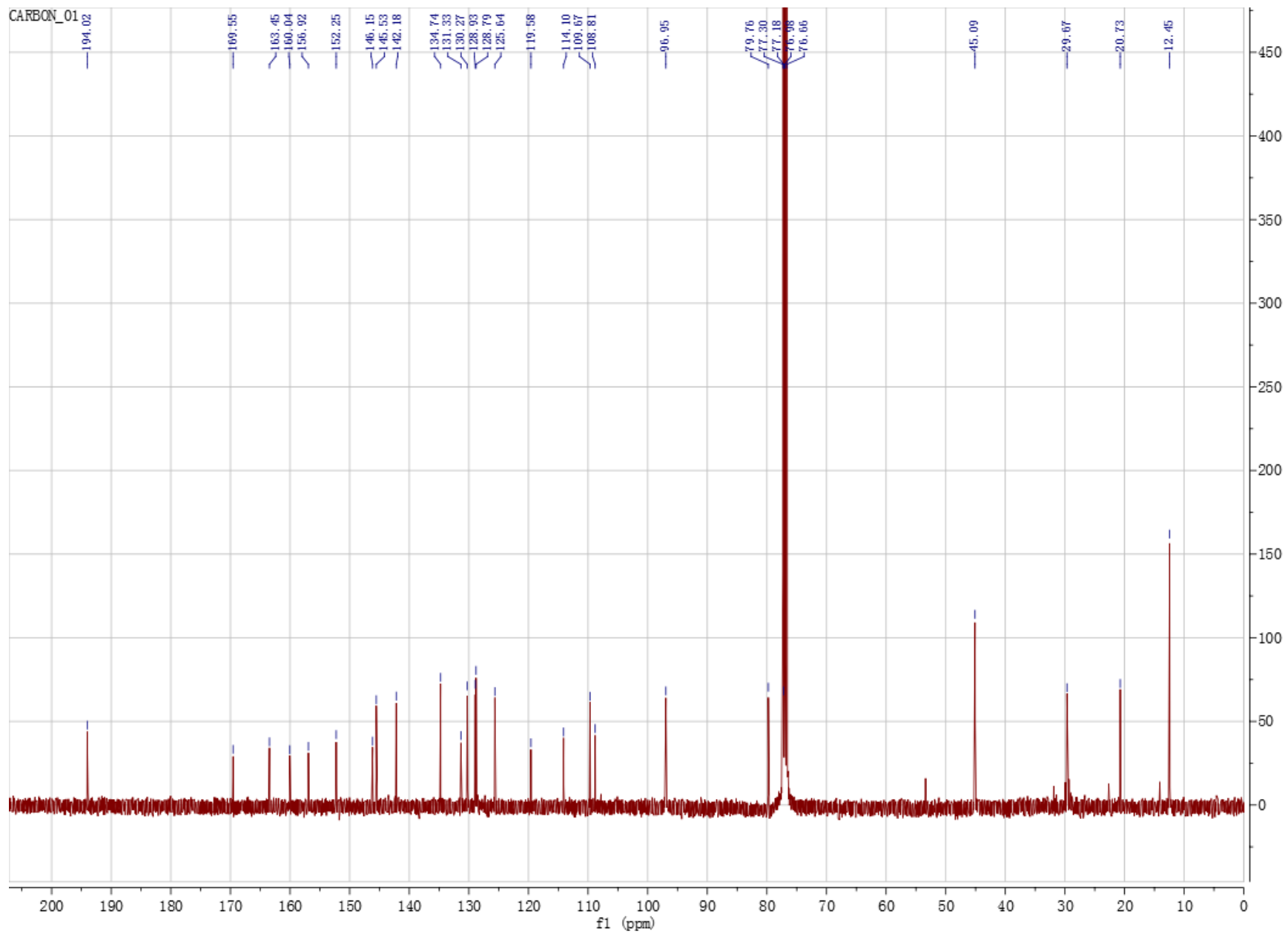


Figure S11. <sup>1</sup>H-NMR (400 MHz, CDCl<sub>3</sub>) spectrum of ThiolQuant Green-AM.



**Figure S12.**  $^{13}\text{C}$ -NMR (100 MHz,  $\text{CDCl}_3$ ) spectrum of ThiolQuant Green-AM.